P516761.PDF [Page: 3 of 37]

DEFENCE R&D DÉFENSE

# Comparison of Three-Dimensional and Axisymmetric Software for Predicting Acoustic Target Strength

*L E Gilroy, J Fawcett*

**Defence R&D Canada**

Technical Memorandum

DREA TM 2001-018

November 2001

National Defence Défense nationale

Canada

P516761.PDF [Page: 4 of 37]

104-06994/

# Comparison of Three-Dimensional and Axisymmetric Software for Predicting Acoustic Target Strength

L.E. Gilroy, J. Fawcett

**Defence Research Establishment Atlantic**

Technical Memorandum

DREA TM 2001-018

November 2001

P516761.PDF [Page: 5 of 37]

Author

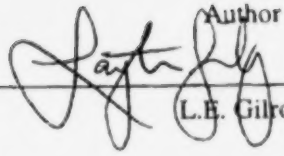

L.E. Gilroy

Approved by

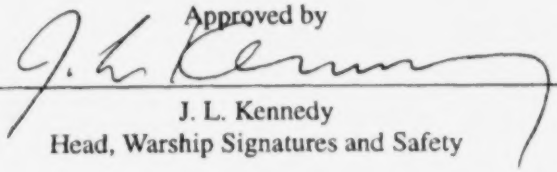

J. L. Kennedy
Head, Warship Signatures and Safety

Approved for release by

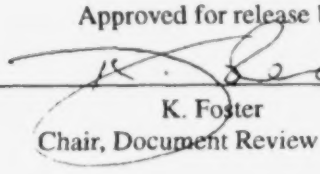

K. Foster
Chair, Document Review Panel

© Her Majesty the Queen as represented by the Minister of National Defence, 2001

© Sa majesté la reine, représentée par le ministre de la Défense nationale, 2001

P516761.PDF [Page: 6 of 37]


## Abstract

Recent work at the Defence Research Establishment Atlantic (DREA) has led to the development of software for predicting the target strength of underwater objects. This capability is incorporated into the general acoustic radiation prediction software tool, AVAST. While AVAST has been successfully validated against a limited set of theoretical data, it has not been fully validated against experimental data or other numerical codes. In this report, AVAST predictions are compared to those made by an axisymmetric-based code (ASBIEM) developed at SACLANTCEN for small cylinders with either flat or hemispherical endcaps. The results were compared at three frequencies for the full monostatic case and the bistatic case (with three different source locations). For the bistatic case, there was generally good agreement between AVAST, ASBIEM, and theoretical results for the specific source locations selected. The results from the cylinder with hemispherical endcaps showed slightly better agreement than those from the flat end cylinder. For the monostatic analyses, the AVAST and ASBIEM codes showed very good agreement at the lower frequencies for both cylinder models. At the lowest frequency, AVAST seemed to show a slightly better agreement with the theoretical results. At the highest frequency, however, AVAST, while correctly matching the broadside and endfire results and the general level, appears to contain some anomalous side lobes and nulls. In general, the comparisons showed that AVAST and ASBIEM gave comparable results when used to predict rigid target strength. The ASBIEM code runs on the order of one magnitude faster than the AVAST code, but cannot be used to model structures which are not axisymmetric.



## Résumé

Des travaux récents effectués au Centre de recherches pour la Défense Atlantique (CRDA) ont conduit à l'élaboration d'un logiciel pour la prévision de l'intensité de cibles sous-marines. Cette capacité est incorporée à l'outil logiciel général de prévision du rayonnement acoustique, AVAST. Ce logiciel a été validé avec succès pour un ensemble limité de données théoriques, mais il n'a pas été entièrement validé pour des données expérimentales ou pour d'autres codes numériques. Dans ce rapport, les prévisions fournies par AVAST sont comparées aux prévisions obtenues avec un logiciel basé sur des structures axisymétriques (ASBIEM) élaboré au SACLANTCEN pour de petits cylindres à bouchons d'extrémités plats ou hémisphériques. On a comparé les résultats obtenus à trois fréquences pour le cas entièrement monostatique et pour le cas bistatique (avec trois emplacements différents de la source). Pour le cas bistatique, l'accord était généralement bon entre les résultats donnés

516761.PDF [Page: 7 of 37]

par AVAST, les résultats donnés par ASBIEM et les résultats théoriques pour les emplacements choisis de la source. L'accord des résultats obtenus avec le cylindre à bouchons d'extrémités hémisphériques était légèrement supérieur à celui obtenu avec le cylindre à bouchons d'extrémités plats. Dans le cas des analyses monostatiques, les logiciels AVAST et ASBIEM ont donné un très bon accord aux fréquences inférieures pour les deux types de cylindres. À la plus basse fréquence, AVAST semblait donner un accord légèrement supérieur avec les résultats théoriques. À la plus haute fréquence, cependant, AVAST, même s'il donnait des résultats en accord avec ceux obtenus pour un rayonnement transversal et un rayonnement longitudinal, de même que pour le niveau général, semblait contenir certains lobes latéraux et creux anormaux. En général, les comparaisons ont montré que les logiciels AVAST et ASBIEM donnaient des résultats comparables lorsqu'ils étaient utilisés pour prévoir l'intensité des cibles rigides. L'exécution du logiciel ASBIEM est d'un ordre de grandeur plus rapide que celle du logiciel AVAST, mais elle ne permet pas de modéliser les structures non axisymétriques.

# Executive summary

## Introduction

An important piece of information in the detection and localization of underwater objects is their acoustic target strength. The likely targets can range in size from ships and submarines to sea mines over a broad range of frequencies. For simple geometric shapes (e.g., spheres, infinite cylinders) and structural compositions (e.g., rigid walls) theoretical target strength solutions exist and are used to approximate the behaviour of real targets. However, these approximations are of limited use if the object is sufficiently complex. For some targets, such as submarines, some experimental data exist, but the measurements are rarely applicable across all submarines. Thus, numerical methods which can be used over a wide range of structures, frequencies, and environmental conditions to predict acoustic target strength are valuable tools for the sonar analyst. A variey of numerical methods are available with most being based on either the finite element or boundary element method.

Recent work at DREA has led to the development of a mixed finite element and boundary element acoustic radiation prediction software tool, AVAST, which can be used to predict the acoustic target strength of full three-dimensional underwater structures. Also, in a separate program at SACLANTCEN, an axisymmetric boundary element-based code, ASBIEM, was developed to investigate the rigid target strength characteristics of mine-like targets over a large frequency range. In the work done at SACLANTCEN, rigid target strength predictions were made for two mine-like targets, each a cylinder of overall length of 2.0m and radius of 0.25m, one with flat endcaps and one with hemispherical endcaps. In this technical memorandum, the theoretical background to the two computer codes are discussed and then both methods are used to predict the target strength for the small 2m cylinders at three different frequencies with a variety of source locations and the results are compared to each other and to selected theoretical results. Results were generated for both the bistatic and full monostatic cases.

## Principal Results

For the bistatic case, there was generally good agreement between AVAST, ASBIEM, and theoretical results for the specific source locations selected. The results from the cylinder with hemispherical endcaps seem to show better agreement than those from the flat end cylinder. The dominant feature of the bistatic target strength in general was forward scattering which was always the largest amplitude lobe.

For the monostatic analyses, the AVAST and ASBIEM codes showed very good

P516761.PDF [Page: 9 of 37]

agreement for both the 2.5 kHz and 5 kHz cases for both cylinder models. At the lowest frequency, AVAST seemed to show a slightly better agreement with the theoretical results. At the highest frequency, however, AVAST, while correctly matching the broadside and endfire results and the general level, appears to contain some anomalous side lobes and nulls.

## Significance of Results

In general, the above comparisons show that AVAST and ASBIEM give comparable results when used to predict rigid target strength. The ASBIEM code runs on the order of one magnitude faster than the AVAST code, but cannot be used to model structures which are not axisymmetric. At the highest frequency in the monostatic case, AVAST predicted a few apparently anomalous side lobes and nulls. In past analyses, these side lobes disappear when a more refined grid is used, so while the bistatic results implied the grid was sufficiently refined, these results indicate this was not the case. At least for the AVAST code, ten elements per acoustic wavelength is not quite sufficient for the complete analysis.

## Future Plans

AVAST supports a number of capabilities not explored in this report which may be of further interest to those involved in submarine detection or mine countermeasures. Issues such as target strength prediction in shallow water including the effects of the bottom and the water surface, and target strength of partially buried mines can be examined using the existing software. Future work on AVAST will concentrate on such things as examining elastic target strength (allowing for internal structure), exploring ways to increase the frequency range (including examining the anomalous lobes demonstrated here), and examining a variety of environmental conditions such as shallow water and varying bottom conditions.

L.E. Gilroy, J. Fawcett; 2001; Comparison of Three-Dimensional and Axisymmetric Software for Predicting Acoustic Target Strength; DREA TM 2001-018; Defence Research Establishment Atlantic.

P516761.PDF [Page: 10 of 37]

# Sommaire

## Introduction

Un élément d'information important dans la détection et la localisation de cibles sous-marines est leur intensité acoustique. Les cibles probables peuvent avoir des tailles allant de celle des navires et des sous-marins à celle des mines marines sur une vaste gamme de fréquences. Pour les formes géométriques simples (p. ex. sphères, cylindres infinis) et les éléments de structure (p. ex. murs rigides) il existe des solutions pour l'intensité des cibles théoriques et elles sont utilisées pour obtenir une approximation du comportement des cibles réelles. Cependant, ces approximations sont d'utilisation limitée lorsque l'objet est assez complexe. Pour certaines cibles, par exemple les sous-marins, il existe certaines données expérimentales, mais les mesures sont rarement applicables à tous les sous-marins. Par conséquent, les méthodes numériques qui peuvent être utilisées pour une vaste gamme de structures, fréquences et conditions environnementales en vue de prévoir l'intensité acoustique des cibles sont des outils précieux pour le spécialiste de l'analyse sonar. Une variété de méthodes numériques sont disponibles, et la plupart sont basées soit sur la méthode par éléments finis, soit sur la méthode par éléments frontières.

Des travaux récents du CRDA ont conduit à l'élaboration d'un outil logiciel de prévision du rayonnement acoustique combinant la méthode par éléments finis et la méthode par éléments frontières, AVAST, qui permet de prévoir l'intensité acoustique de structures sous-marines entièrement tridimensionnelles. De plus, dans le cadre d'un programme distinct mené au SACLANTCEN, un logiciel basé sur des éléments frontières axisymétriques, ASBIEM, a été élaboré pour l'étude des caractéristiques d'intensité de cibles rigides semblables à des mines sur une vaste gamme de fréquences.

Dans le cadre des travaux effectués au SACLANTCEN, des prévisions de l'intensité de cibles rigides ont été faites pour deux cibles semblables à des mines, consistant chacune en un cylindre ayant une longueur hors tout de 2,0 m et un rayon de 0,25 m, une à bouchons d'extrémités plats, l'autre à bouchons d'extrémités hémisphériques. Dans ce document technique, on traite du contexte théorique des deux logiciels, puis on utilise les deux méthodes pour prévoir l'intensité des petits cylindres cibles de 2 m à trois fréquences différentes avec une variété d'emplacements de la source et on compare les résultats entre eux et à des résultats théoriques choisis. Des résultats ont été obtenus pour le cas bistatique et le cas entièrement monostatique.

P516761.PDF [Page: 11 of 37]

## Principaux résultats

Pour le cas bistatique, l'accord était généralement bon entre les résultats donnés par AVAST, les résultats donnés par ASBIEM et les résultats théoriques pour les emplacements choisis de la source. L'accord des résultats obtenus avec le cylindre à bouchons d'extrémités hémisphériques était légèrement supérieur à celui obtenu avec le cylindre à bouchons d'extrémités plats. La caractéristique dominante de l'intensité de cible bistatique en général était la diffusion vers l'avant, qui était toujours le lobe de plus grande amplitude.

Dans le cas des analyses monostatiques, AVAST et ASBIEM ont donné un très bon accord à 2,5 kHz et à 5 kHz pour les deux types de cylindres. À la plus basse fréquence, AVAST semblait donner un accord légèrement supérieur avec les résultats théoriques. À la plus haute fréquence, cependant, AVAST, même s'il donnait des résultats en accord avec ceux obtenus pour un rayonnement transversal et un rayonnement longitudinal, de même que pour le niveau général, semblait contenir certains lobes latéraux et creux anormaux.

## Signification des résultats

En général, les comparaisons susmentionnées montrent que les logiciels AVAST et ASBIEM donnent des résultats comparables lorsqu'ils sont utilisés pour prévoir l'intensité de cibles rigides. L'exécution du logiciel ASBIEM est d'un ordre de grandeur plus rapide que celle du logiciel AVAST, mais elle ne permet pas de modéliser les structures non axisymétriques. À la plus haute fréquence du cas monostatique, AVAST prévoyait quelques lobes et creux apparemment anormaux. Dans les analyses antérieures, ces lobes latéraux disparaissaient lorsqu'on utilisait un quadrillage plus perfectionné. Par conséquent, même si les résultats du cas bistatique laissaient sous-entendre que le quadrillage était suffisamment perfectionné, les nouvelles données indiquent qu'il ne l'était pas. Pour AVAST au moins, il n'est pas tout à fait suffisant d'utiliser dix éléments par longueur d'onde acoustique pour l'analyse complète.

## Plans futurs

AVAST permet un certain nombre de fonctions qui ne sont pas étudiées dans ce rapport et qui peuvent intéresser davantage les responsables de la détection des sous-marins et de la lutte contre les mines. Les questions telles que la prévision de l'intensité des cibles en eaux peu profondes, y compris les effets du fond et de la surface de l'eau, et de l'intensité des mines partiellement enfouies peuvent être étudiées à l'aide du logiciel actuel. Les travaux futurs relatifs à AVAST seront axés sur des aspects tels que l'étude de l'intensité des cibles élastiques (tenant compte de

P516761.PDF [Page: 12 of 37]

la structure interne), la recherche de moyens pour accroître la plage de fréquences (y compris l'étude des lobes anormaux observés) et l'étude d'une variété de conditions environnementales, par exemple les conditions d'eaux peu profondes et de fonds variables.

L.E. Gilroy, J. Fawcett; 2001; Comparison of Three-Dimensional and Axisymmetric Software for Predicting Acoustic Target Strength; DREA TM 2001-018; Centre de recherches pour la défense Atlantique.

P516761.PDF [Page: 13 of 37]

# Table of contents

Abstract . . . . . i

Résumé . . . . . i

Executive summary . . . . . iii

Sommaire . . . . . v

Table of contents . . . . . viii

1 Introduction . . . . . 1

2 AVAST . . . . . 2

3 ASBIEM . . . . . 4

4 Theoretical Target Strength . . . . . 5

5 Numerical Models . . . . . 7

6 Results . . . . . 9

6.1 Bistatic Target Strength . . . . . 9

6.2 Monostatic Target Strength . . . . . 16

7 Conclusions . . . . . 16

References . . . . . 20

P516761.PDF [Page: 14 of 37]

# 1 Introduction

The ability to predict the target strength of underwater objects is of great interest to the sonar community to assist in target localization and identification. Numerical methods of target strength prediction are useful as experimental measurements of target strength are difficult to perform and cannot easily cover the range of conditions available to numerical methods. A variey of numerical methods are available with most being based on either the finite element or boundary element method.

Recent work in support of the Ship Noise Project at the Defence Research Establishment Atlantic (DREA) has led to the development of a mixed finite element and boundary element acoustic radiation prediction software tool, AVAST [1, 2, 3, 4]. This software originally was used to predict the low frequency radiated noise from submerged or floating elastic structures and is intended to assist DND in either optimizing the structural arrangement to minimize radiated noise or in examining existing structures to isolate noise sources. During the development of the software, a capability to predict scattered sound pressure (given an external source) was also implemented. This capability allowed for both a rigid structure and an elastic structure assuming that a natural frequency analysis of the structure could be performed up to the required frequency. Given the existing scattering capability, a target strength prediction capability was a relatively simple addition to the AVAST software. As with the scattering problem, AVAST can solve both the rigid and elastic target cases, however further investigation is required to determine if a sufficiently large range of frequencies can be accommodated for the elastic target case. AVAST has a full 3D capability, so can it be used to examine complex asymmetric structures. However, AVAST does not have an axisymmetric capability and, thus, requires a much larger model for such targets than would be required with a purely axisymmetric code.

In support of the project on Modelling Scattering from Buried Objects, an axisymmetric boundary element-based (ASBIEM) program, was developed at SACLANTCEN [5]. The program was used to investigate the rigid and elastic target strength characteristics of mine-like targets over a large frequency range. The advantage of such a program is the capability to cover a very large frequency range with relatively few elements (as one is only required to model the 2D shape of the target using line elements). The primary disadvantage of such a program is the restriction to axisymmetric geometries.

Initial target strength work with AVAST has involved the prediction of rigid target strength for a variety of targets focussed on submarine-based models, including large cylinders and more realistic submarine shapes [6, 7, 8]. In the work done at SACLANTCEN, rigid target strength predictions were made for two mine-like targets, each a cylinder of overall length of 2.0m and radius of 0.25m, one with

flat endcaps and one with hemispherical endcaps. In this technical memorandum, the theoretical background to the two computer codes are discussed and then both methods are used to predict the target strength for the small 2m cylinders at three different frequencies (2.5 kHz, 5.0 kHz, and 7.5 kHz) with a variety of source locations and the results are compared to each other and to selected theoretical results.

# 2 AVAST

Under contract to DREA, Martec Ltd. has developed a series of computer programs, collectively named AVAST, for use in the numerical prediction of the acoustic radiation and scattering from floating or submerged elastic structures immersed in either infinite, half-space or finite depth fluid domains. More recently, the modelling capabilities of the AVAST code have been extended to include target strength analysis of both elastic and inelastic structures. AVAST combines both the finite element method for the structure and the boundary integral equation technique for the fluid. Note that, for a rigid target, a structural finite element model is not required, it is simply necessary to model the shape of the wetted surface of the structure.

For problems involving exterior fluid domains, AVAST employs a boundary element formulation based upon the classical Helmholtz integral equation, i.e.:

$$c_g(P_f)\, p(P_f) = \int_S \left[ G(P_f, Q)\rho\omega^2 u(Q) - \frac{\partial G(P_f, Q)}{\partial n_Q} p(Q) \right] dS(Q) + 4\pi p_i(P_f) \tag{1}$$

where $G$ represents the Green's function due to a harmonic point source located at point Q, $p(P_f)$ represents the acoustic pressure at a point $P_f$ in the fluid domain (satisfying the Helmholtz differential equation for time-harmonic waves, $\nabla^2 p(P_f) + k^2 p(P_f) = 0$), $\omega$ represents the angular frequency, $\rho$ represents the fluid density, $u(Q)$ represents the displacement amplitude normal to the body surface $S$ at the point $Q$, $p_i(P_f)$ represents the prescribed pressure of the incident acoustic wave, and $n_Q$ represents the surface normal vector at point $Q$.

For the special case of a body submerged in an infinite fluid domain, this Green's function can be expressed using the following formula:

$$G(P_f, Q) = \frac{e^{-ikR(P_f,Q)}}{R(P_f, Q)} \tag{2}$$

where $R$ is the distance between $P_f$ and $Q$ and $k$ represents the acoustic wavenumber $(\omega/c)$, where $c$ represents the fluid sound speed. In addition, the coefficient $c_g(P_f)$ is a function of the local geometry, having a value of $4\pi$ for locations $P_f$ fully immersed in the fluid domain and a value of $2\pi$ for points residing on the body surface.

In order to solve the integral formulation posed above in Equation 1, a four-step numerical technique was developed and implemented into the AVAST code. The first step involves the discretization of the wet surface of the underwater target into a collection of either 3-node or 4-node boundary element panels. Step two involves the numerical integration of Helmholtz integral equation over the surface of the body (represented by the boundary element panels). This leads to a system of algebraic equations relating the acoustic pressure on the surface of the body to the incident pressure field and surface normal velocities, i.e.:

$$[H]\{p\} = [G]\{u\} + \{p_i\} \tag{3}$$

where the number of unknown surface pressures (length of the vector $\{p\}$) is equal to the number of boundary element panels and the matrix operators $[H]$ and $[G]$ can be expressed using the following forms:

$$G_{ij} = \int_{S_j} G(P_{f_i}, Q_j) dS_j \tag{4}$$

and

$$H_{ij} = \int_{S_j} \frac{\partial G(P_{f_i}, Q_j)}{\partial n_{Q_j}} dS_j \tag{5}$$

where the subscripts $ij$ represent the $i$-th row and the $j$-th column of the matrices $[H]$ and $[G]$.

The third step in the AVAST solution procedure involves solving Equation 3 for the surface acoustic pressures, i.e.:

$$\{p\} = [H]^{-1}\left(\rho\omega^2 [G]\{u\} + \{p_i\}\right) \tag{6}$$

These surface acoustic pressures can also be expressed in terms of nodal forces, $\{f_A\}$ (on the structure), i.e.:

$$\begin{aligned} \{f_A\} &= [T]^T [A]\{p_i\} \\ &= \rho\omega^2 [T]^T [A][H]^{-1}[G][T]\{x\} + [T]^T [A][H]^{-1}\{p_i\} \\ &= \omega^2 [M_f]\{x\} + [T]^T [A][H]^{-1}\{p_i\} \end{aligned} \tag{7}$$

where $[T]$ represents a transformation matrix relating the global cartesian structural degrees of freedom to the boundary element panel normals, $[A]$ represents a diagonal fluid panel area matrix, $[M_f]$ represents the so-called acoustic fluid mass matrix, and $\{x\}$ represents a vector of body displacements defined in terms of the global coordinate system.

In the fourth and final stage of an AVAST solution technique the surface acoustic pressures, computed during the third phase, are used to predict the sound pressure

levels at points residing in the fluid domain. Once these *field pressures* have been computed, estimates of the body's target strength can be generated using Equation 16.

AVAST models can be imported from a number of sources including some standard mesh generation packages. Using the AVAST GUI, sources, field points, wave guides, free surfaces, fluid properties, etc. may be added to the model which is then solved at specified frequencies or ranges of frequencies. Results may be plotted in the AVAST GUI or exported.

# 3 ASBIEM

The azimuthally-symmetric Boundary Integral Equation Method (ASBIEM) starts from the three-dimensional integral equation for the pressure on a rigid object, following the form of Eq.(1) (with velocities, $u$, set to zero as it is a rigid object)

$$p = -\frac{1}{4\pi}\int_S \frac{\partial G(r_f, z_f, r_Q, z_Q, \theta_f - \theta_Q)}{\partial n_Q} dS(Q) + p_i \tag{8}$$

Here a cylindrical coordinate system is used; the object is assumed to be azimuthally-symmetric about the $z$-axis; the angle $\theta$ is the polar angle around the $z$-axis. The Green's function itself depends only on the difference of the field angle $\theta_f$ and the integration angle $\theta_Q$. To exploit the angular symmetry of the problem, the pressure field $p(r_f, z_f, \theta_f)$ is expanded in a Fourier series with unknown coefficients $p_m(r, z)$,

$$p(r_f, z_f, \theta_f) = \sum_{m=-\infty}^{\infty} p_m(r_f, z_f) e^{im\theta}. \tag{9}$$

Similarly,

$$p_i = \sum_{m=-\infty}^{\infty} i_m(r_f, z_f) e^{im\theta} \tag{10}$$

where in this case the incident coefficients are known. The Green's function or its normal derivative can also be expanded in the form,

$$\frac{\partial G(P_f, Q)}{\partial n_q} = \sum_{m=-\infty}^{\infty} g_m(r_f, z_f, r_Q, z_q) e^{im\tau} \tag{11}$$

where

$$g_m(r_f, z_f, r_q, z_q) \equiv \frac{1}{2\pi}\int_{-\pi}^{\pi} G(r_f, z_f, r_Q, z_q, \tau) e^{im\tau} d\tau \tag{12}$$

and $\tau \equiv \theta_f - \theta_Q$. In fact since $G(r_f, z_f, r_Q, z_Q, \tau) = G(r_f, z_f, r_Q, z_Q, -\tau)$, Eq(12) can be rewritten as

$$g_m(r_f, z_f, r_q, z_q) \equiv 2 \int_0^\pi G(r_f, z_f, r_Q, z_q, \tau) \cos(m\tau) d\tau. \tag{13}$$

Using the series expressions in Eq.(8) it is not difficult to obtain the integral relations for the coefficient $p_m(r_f, z_f)$ on the object,

$$p_m = \int_\Omega 2\pi g_m(r_f, z_f, r_Q, z_q) p_m(r_q, z_q) d\Omega + i_m \tag{14}$$

where $\Omega$ is the $(r_Q, z_Q)$ domain of integration. Once having solved for $p_m$, the field can be computed at an arbitrary field point $(r_f, z_f)$ off the scattering object using the Helmholtz integral of Eq.(8); then the true scattered pressure value at this point can be computed by

$$p(r_f, z_f, \theta) = \sum_{m=-\infty}^{\infty} p_m(r_f, z_f) e^{im\theta} = \sum_{m=0}^{\infty} \epsilon_m p_m(r_f, z_f) \cos m\theta \tag{15}$$

where $\epsilon_m = 1$ for $m = 0$ and $\epsilon_m = 2$ otherwise.

The computational advantage to this Fourier decomposition is that a full three-dimensional problem has been reduced to solving a sequence of much-smaller two-dimensional problems.

For this program, the geometric models of the cylinders have been hard-wired into the software. At program runtime, the structural configuration (whether flat or hemispherical ends) and dimensions (overall length and radius) may be seleceid.

# 4 Theoretical Target Strength

Target strength ($TS$) is defined [9, 10] as the ratio, on a decibel scale, of the acoustic intensity ($I_s$) scattered in a particular direction to the incident acoustic intensity ($I_i$) where the scattered and incident intensities are determined at unit distance from the acoustic center of the target. Alternatively, the intensity parameters may be replaced by expressions for pressure ($p$) under the far-field approximation which leads to the following expression for target strength,

$$TS = 20 \log\left(\frac{p_s}{p_i}\right) + 20 \log\left(\frac{r}{r_o}\right) \tag{16}$$

where $p_s$ represents the scattered pressure and $p_i$ represents the incident acoustic pressure. Note that the scattered pressure is measured at a specific location in the

far field while the incident pressure is that measured at the target location. This equation also contains the term to correct to the reference measurement distance of one unit of length ($r_o$, usually 1m). This correction, based on the assumption of spherical spreading, is made to account for the relative position of the measurement point with respect to the acoustic center of the target, i.e.: where $r$ represents the distance between the field point and the acoustic center of the target.

For *monostatic* target strength, the measurement field point or sonar receiver position lies in the direction back towards the source location and the scatter is referred to as *backscatter*. For *bistatic* target strength, the measurement point may lie in any direction relative to the target. Of some interest is the scattered response directly opposite the target from the source, which is known as *forward scatter*.

In this type of analysis, the non-dimensional frequency $ka$ is frequently used, where (for acoustic wavelength $\lambda$)

$$k = \frac{2\pi}{\lambda} \tag{17}$$

and $a$ is a representative dimension of the target (typically radius for spheres and cylinders).

The theoretical solution for the monostatic target strength of a finite cylinder of radius $a$ and length $L$ is given [11] as:

$$\mathrm{TS} = 10\ log\left(\frac{aL^2}{2\lambda}\right) \tag{18}$$

which is valid for

$$ka >> 1\ ,\quad r > \frac{L^2}{\lambda} \tag{19}$$

where the source is assumed to be broadside to the cylinder. The analyses in this report were done at frequencies of 2.5, 5, and 7.5 kHz, which correspond to $ka$ values of, respectively, 2.62, 5.24, and 7.86. These $ka$ values then correspond to minimum distances from the cylinder of 6.7m, 13m, and 20m. The field point distance selected was 20m. For the flat-ended cylinder, the above equation results in a target strengths at 1m of 2.2 dB at 5 kHz, -0.8 dB at 2.5 kHz and 4.0 dB at 7.5 kHz. This equation models cylinders with flat endcaps [12] and, thus, would not account for the differences due to the different endcaps. For cylinders with high length-to-radius ratios, any differences should be relatively minor. As the cylinders used in this study were relatively short, the equation may be less accurate for the models with hemispherical endcaps. Also, the lowest frequency used does not strictly match the condition $ka >> 1$.

An approximation to the forward scattered target strength of a cylinder (with the

source broadside) is given [13] as:

$$\mathrm{FTS} = 20\ log\left(\frac{2aL}{\lambda}\right) \tag{20}$$

which results in a FTS of 4.4 dB at 2.5 kHz, 10.5 dB at 5 kHz and 14.0 dB for a frequency of 7.5 kHz. As this equation is based on the projected area of the cylinder, it should more accurate for the cylinder with flat ends.

For the flat end cylinder, the monostatic target strength for the case with the source in line with the end of the cylinder can be approximated by that of a flat plate which is given in [10] as:

$$\mathrm{TS} = 10\ log\left(\frac{A}{\lambda}\right)^2 \tag{21}$$

which is valid for the same range as the cylinder's target strength. In this equation, $A$ is the area of the plate facing the source. This equation results in target strengths of -9.7 dB at 2.5 kHz, -3.7 dB at 5 kHz, and -0.2 dB at 7.5 kHz.

For the cylinder with hemispherical ends, the monostatic target strength for a source on the end of the cylinder can be approximated by that of a sphere which is given in [10] as:

$$\mathrm{TS} = 10\ log\left[\frac{a^2}{4} + \frac{a^2}{4}tan^2\left(\frac{\beta}{2}\right) J_1^2(ka\ sin\beta)\right] \tag{22}$$

which is valid for

$$ka >> 1\ ,\quad r > a \tag{23}$$

where $J_1$ is a Bessel function of order 1 and $\beta$ is the bistatic angle between the direction of the incident wave and the scattered wave (which is 0° for backscatter). For all three frequencies, this results in a monostatic target strength of -18.1 dB . If the formula is used to calculate the forward scattered target strength, it results in values of -9.1 dB, -3.5 dB, and -0.11 dB for, respectively, 2.5 kHz, 5 kHz, and 7.5 kHz.

# 5 Numerical Models

As stated above, two different cylinders were examined in this study. Each had an overall length of 2.0m and a radius of 0.25m. As the study only involved the prediction of rigid target strength, internal structure was not modelled.

The AVAST models used are shown in Figure 1. Two different models were used for each type of endcap. For the 2.5 kHz case, the flat end cylinder had a total of 4710 panels, while for the higher frequency runs the model used had 9288 panels.

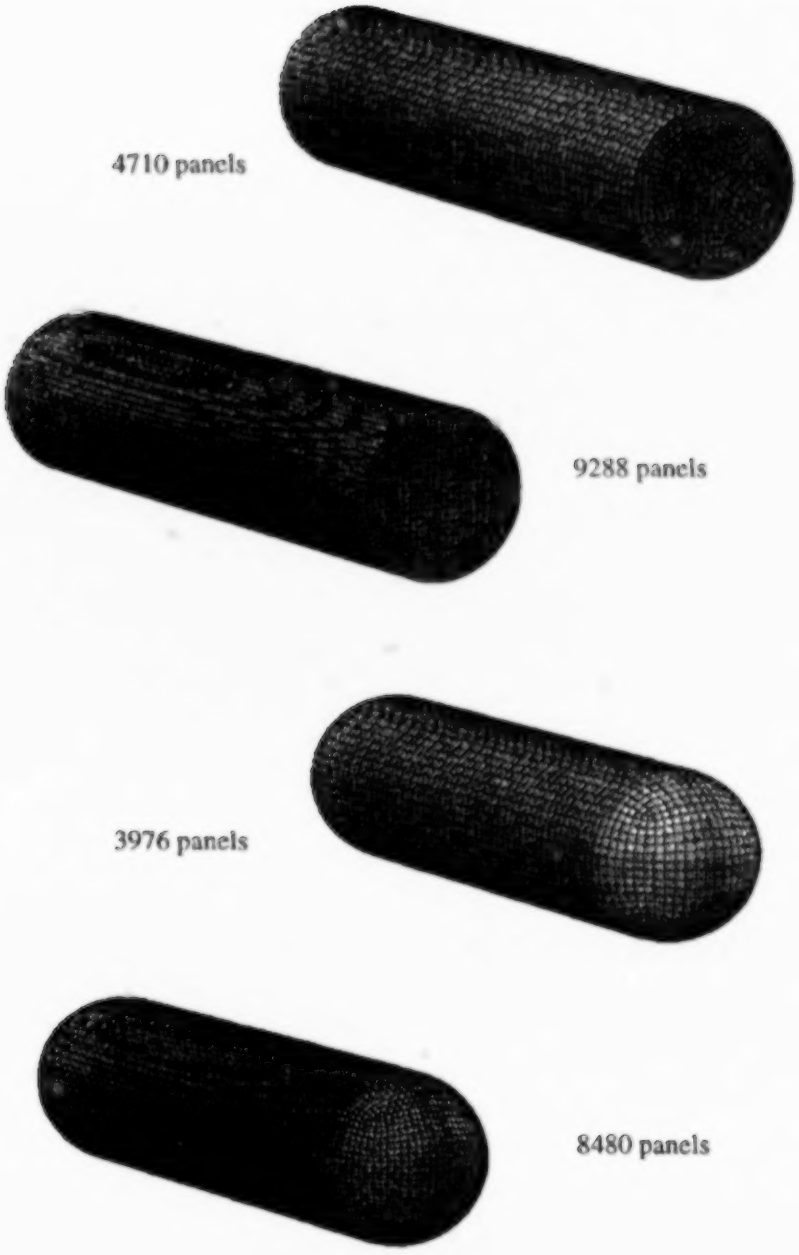


***Figure 1:** AVAST Cylinder Models*

The hemispherical end cylinder model had 3976 panels for the 2.5 kHz run and 8480 panels for the 5 kHz and 7.5 kHz runs. These models resulted in 21 elements per wavelength at 2.5 kHz, 15 at 5 kHz, and 10 at 7.5 kHz. A rule of thumb used in early model development was to insure at least six (four- or three-noded) elements per acoustic wavelength. Early testing showed this level of discretization to be inadequate and subsequent testing showed ten to twelve elements per wavelength to be the minumum level of discretization for reasonable results.

The target strength was predicted using field points at a radius of 20m in a plane coincident with the cylinder axis and a source at a distance of 50m.

For the axisymmetric program, the models were obviously much simpler. The cylinders with hemispherical endcaps were discretized to an average level of approximately 14 elements per wavelength and the cylinders with flat ends to a level of approximately 16 elements per wavelength. This discretization was skewed slightly towards more refined endcaps. The maximum number of elements used was thus 156 at 7.5 kHz. The target strength was calculated with field points at a radius of 10m.

For both programs, the sound speed used was that of sea water (1500 m/s) and the target strength values were corrected to a distance of 1m. Both programs assumed a free-field environment.

# 6 Results

Target strength predictions for both computer codes were made for both the bistatic case and the complete monostatic case (where the monostatic target strength is calculated for every angle of interest and plotted on one curve). Thus, for the bistatic predictions, a single source location was used with field points located on a circle around the target, while for the second case, the source and receiver were moved together around the target.

## 6.1 Bistatic Target Strength

Some representative bistatic target strength patterns calculated by AVAST and the ASBIEM software are shown in Figures 2 to 10. The figures show the calculated bistatic target strength patterns for three source positions at the three different frequencies for the two models. The scale is in dB at 1m.

The first set had the source broadside to the cylinders (90°), the second source was 20° off the cylinders' axes, and the third set shows the target strength with the source

P516761.PDF [Page: 23 of 37]

end-on (90°) to the cylinders. In all the polar plots, the source location is marked with an asterisk (⋆) and any theoretical results are marked with a diamond (⋄).

In general, the figures show good agreement between the AVAST results, the ASBIEM results, and the theoretical results (where available). As expected, the theoretical results gave a better match for the cylinders with flat endcaps. Between the numerical models, the cylinder with hemispherical endcaps seem to show better agreement than those from the flat end cylinder. As well, over the range of frequencies used, the flat-end cylinder target strength typically showed more lobes (was "spikier") than that of the cylinder with hemispherical ends. Both of these results may be due to the sharp geometric change at the flat end which should cause sharper changes in the target strength and which may cause some problems for the numerical codes which, in general, deal better with slightly curving geometries. Typically, the agreement did not degrade with frequency, indicating that the grid refinement appeared to be sufficient even at the highest frequency.

The dominant feature of the target strength with the source broadside was forward scattering with levels typically 5-8 dB higher than the backscatter. Also, there were typically more lobes in the forward scatter direction. With the source at the 20° angle, the largest difference was the lack of an obvious specular reflection from the endcap for the cylinder with hemispherical ends. At all three frequencies, the forward scatter and the specular reflection from the sides of the cylinder gave similar patterns between the two models, however, particularly at the two higher frequencies, there was a large specular reflection from the flat endcap which was not present for the other model. The worst agreement of this set of results appeared to occur for the 7.5 kHz case with the source at 0°. The AVAST results showed strong side lobes at ±20° which did not appear in the ASBIEM results. Note that results for the cylinder with hemispherical ends were indistinguishable from those for a sphere with the same radius.

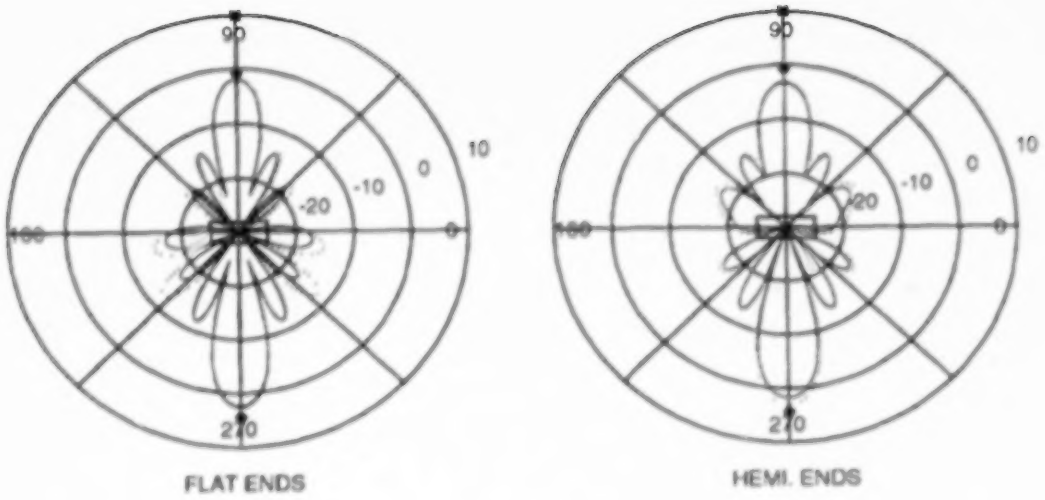


***Figure 2:*** *Bistatic TS at 2.5 kHz - Source Broadside (— AVAST, · · · ASBIEM)*

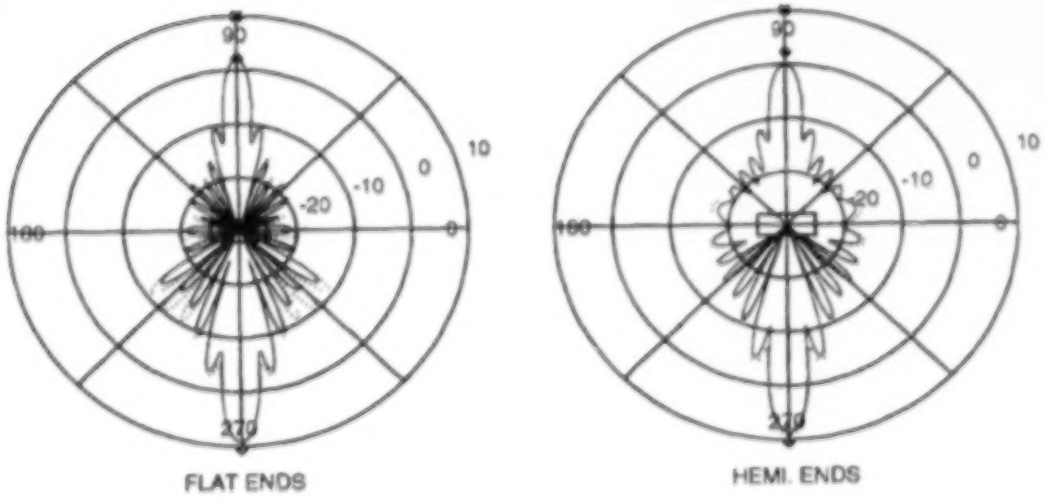


***Figure 3:*** *Bistatic TS at 5 kHz - Source Broadside (— AVAST, · · · ASBIEM)*

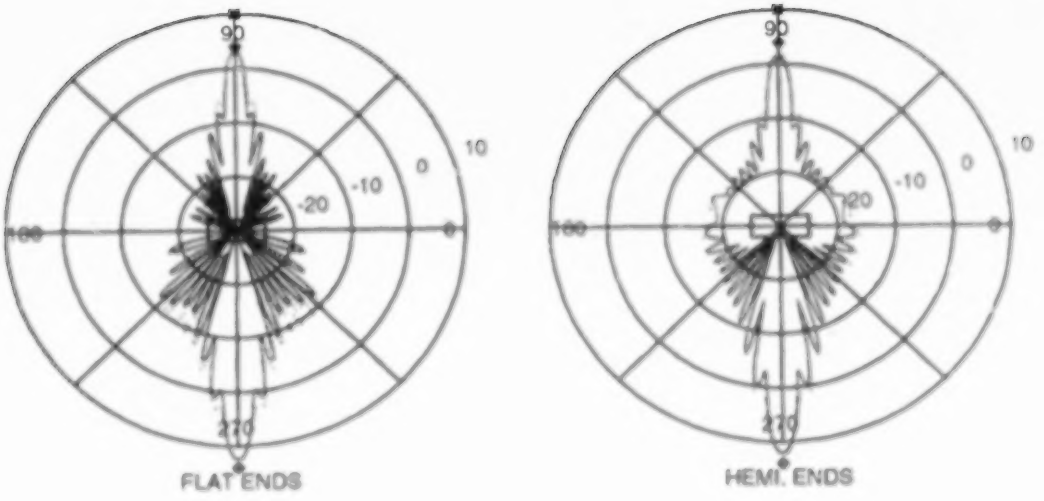


***Figure 4:*** *Bistatic TS at 7.5 kHz - Source Broadside (— AVAST, · · · ASBIEM)*

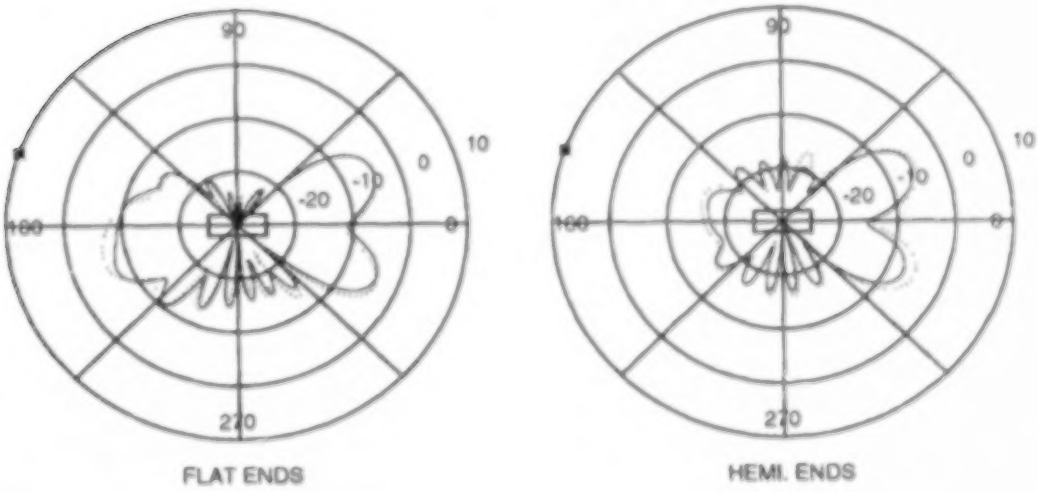


***Figure 5:*** *Bistatic TS at 2.5 kHz - Source Oblique (— AVAST, · · · ASBIEM)*

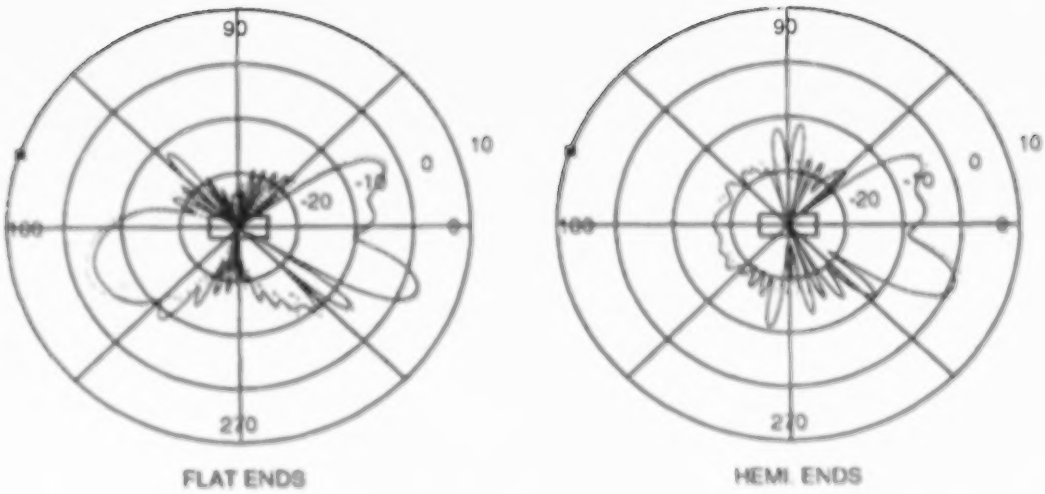


*Figure 6: Bistatic TS at 5 kHz - Source Oblique (— AVAST, · · · ASBIEM)*

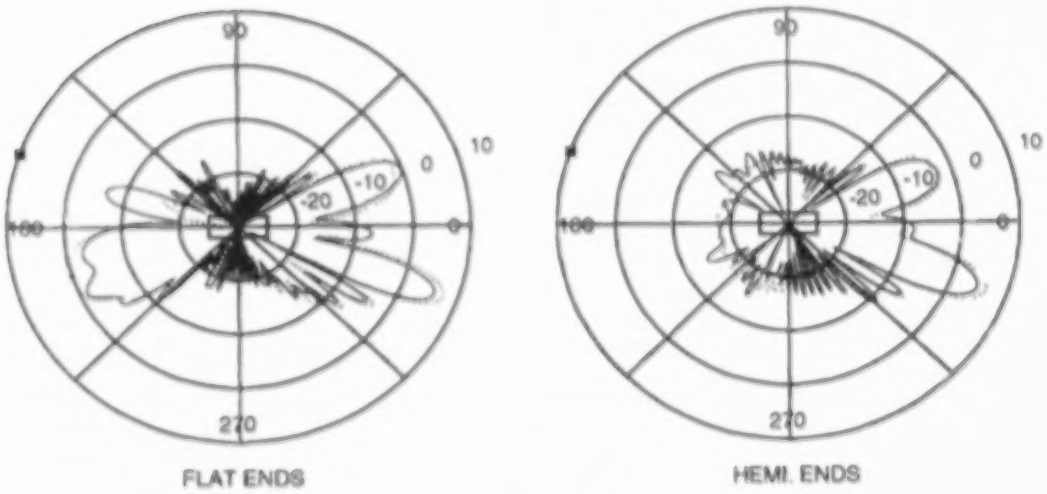


*Figure 7: Bistatic TS at 7.5 kHz - Source Oblique (— AVAST, · · · ASBIEM)*

P516761.PDF [Page: 27 of 37]

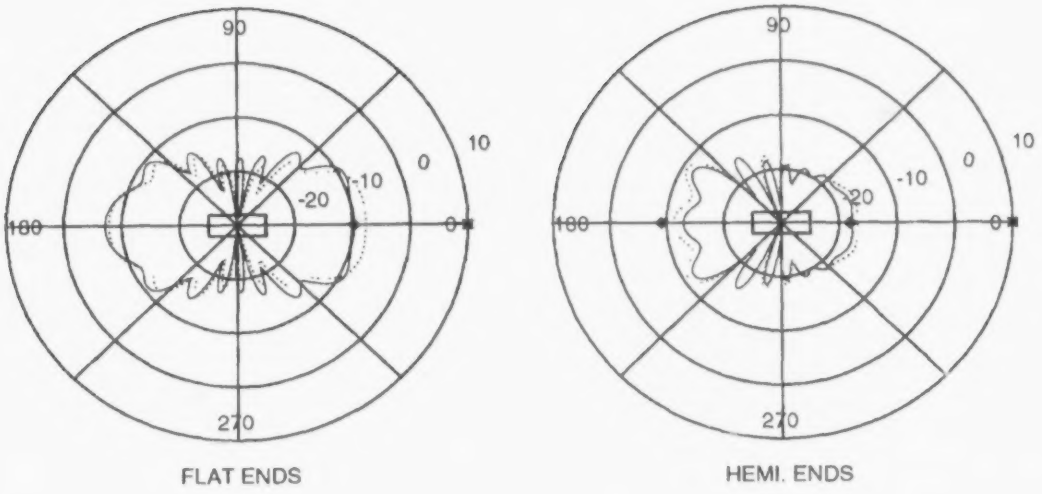


***Figure 8:*** *Bistatic TS at 2.5 kHz - Source on End (— AVAST, · · · ASBIEM)*

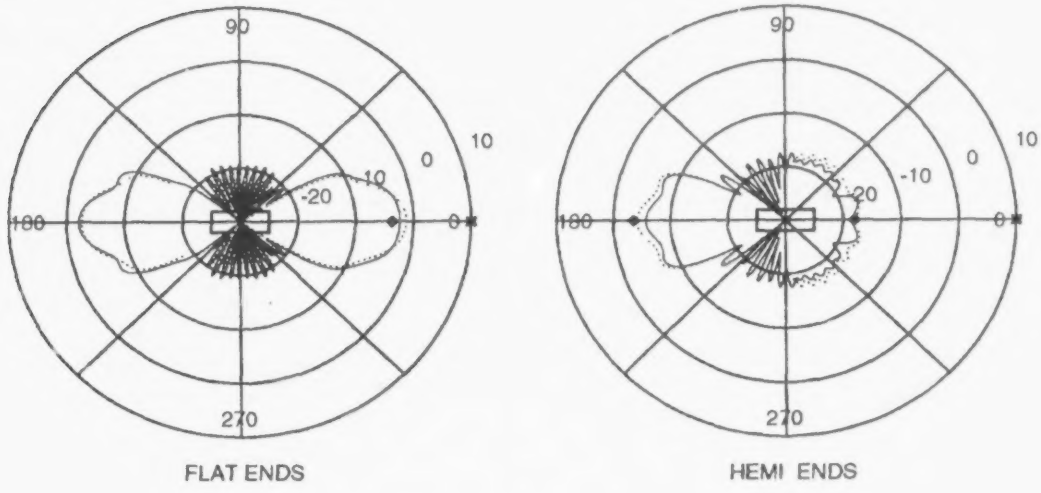


***Figure 9:*** *Bistatic TS at 5 kHz - Source on End (— AVAST, · · · ASBIEM)*

P516761.PDF [Page: 28 of 37]

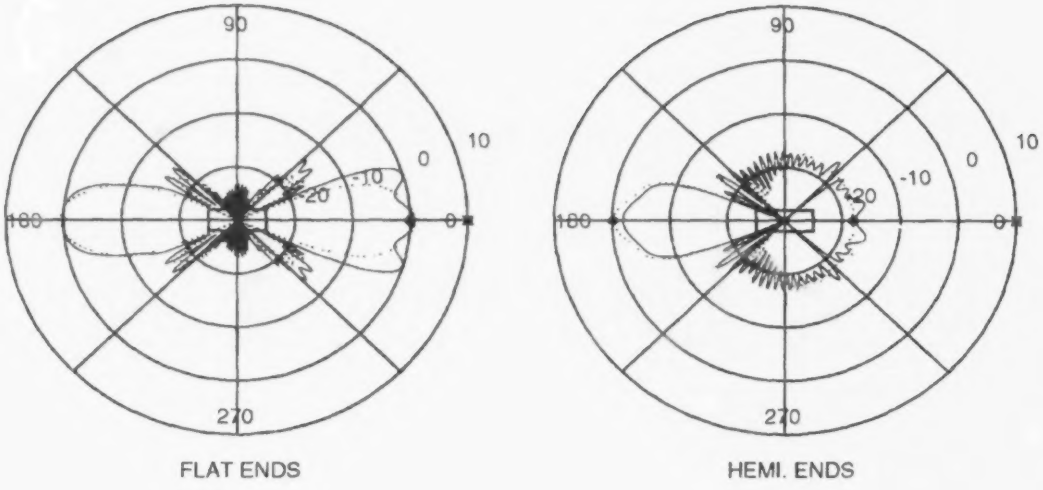


***Figure 10:*** *Bistatic TS at 7.5 kHz - Source on End (— AVAST, · · · ASBIEM)*

## 6.2 Monostatic Target Strength

For each of the models and each of the three frequencies, complete monostatic target strength diagrams were also calculated and are shown in Figures 11 to 16. In this case they are plotted as $X$-$Y$ plots rather than polar plots with 90° being broadside and 0° and 180° being endfire. As the systems were symmetric, only one half the target strength plots are shown. As above, theoretical results are marked with a diamond ($\diamond$).

As can be seen from Figures 11 through 14, the AVAST and ASBIEM codes showed very good agreement for both the 2.5 kHz and 5 kHz cases for both cylinder models. At the lowest frequency, AVAST seemed to show a slightly better agreement with the theoretical results. At the highest frequency (Figures 15 and 16), however, AVAST, while correctly matching the broadside and endfire results and the general level, appears to contain some anomalous large side lobes (at $\pm 15°$ and 25° from broadside) for the flat end cylinder and an oddly deep null (at $\pm 48°$ from broadside) for the cylinder with hemispherical ends. In past analyses, these side lobes disappear when a more refined grid is used. It is not clear at this time what causes these anomalous lobes and it is being pursued. Note that the results appear to match the ASBIEM results at all other locations.

As in the previous section, the results from the cylinder with hemispherical ends showed less variation (from peak to valley) than the flat end cylinder. The flat end cylinder plots show a larger number of peaks and the nulls were typically 5 to 15 dB lower than those of the cylinder with the hemispherical ends. For the exact broadside case, the numerical codes matched the theoretical results better for the flat end cylinder indicating that the theoretical values are best applied to this type of cylinder. Based on a series of runs performed with the ASBIEM code and other AVAST results, the flat-end and hemispherical-end cylinder results seem to converge as the cylinder aspect ratio increases.

# 7 Conclusions

Two separately developed numerical codes for predicting the acoustic target strength of underwater structures were compared using models of mine-sized cylinders at a variety of frequencies. While both programs use the boundary integral equation to solve the target strength problem, AVAST uses full three-dimensional models while ASBIEM deals with only axisymmetric models. While AVAST is capable of solving much more complex structures, by its very nature it will take much longer to solve those problems which can be modelled axisymmetrically (using the same element dimensions).

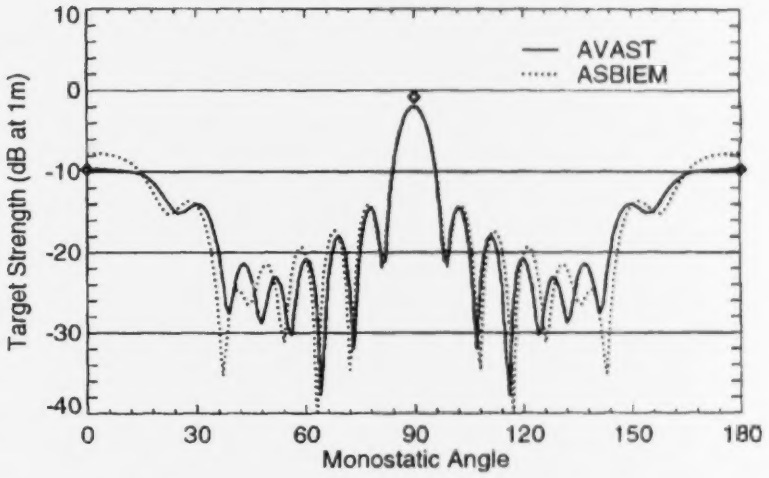


***Figure 11:*** *Monostatic TS of Flat Cylinder - 2.5 kHz*

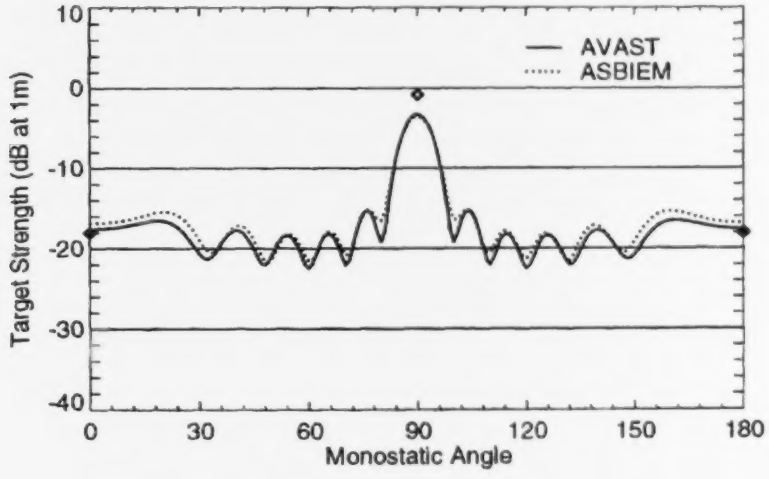


***Figure 12:*** *Monostatic TS of Hemi Cylinder - 2.5 kHz*

P516761 PDF [Page: 31 of 37]

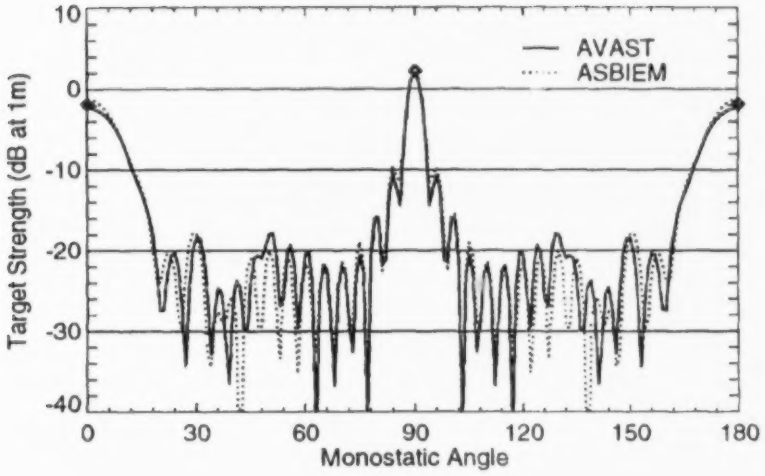


***Figure 13:*** *Monostatic TS of Flat Cylinder - 5 kHz*

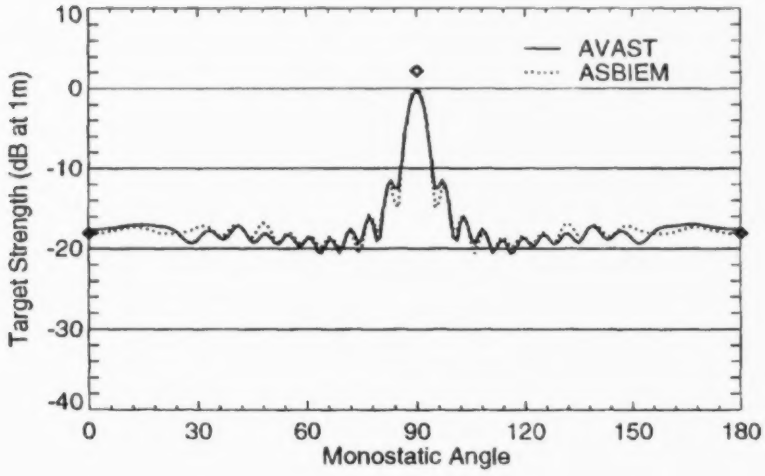


***Figure 14:*** *Monostatic TS of Hemi Cylinder - 5 kHz*

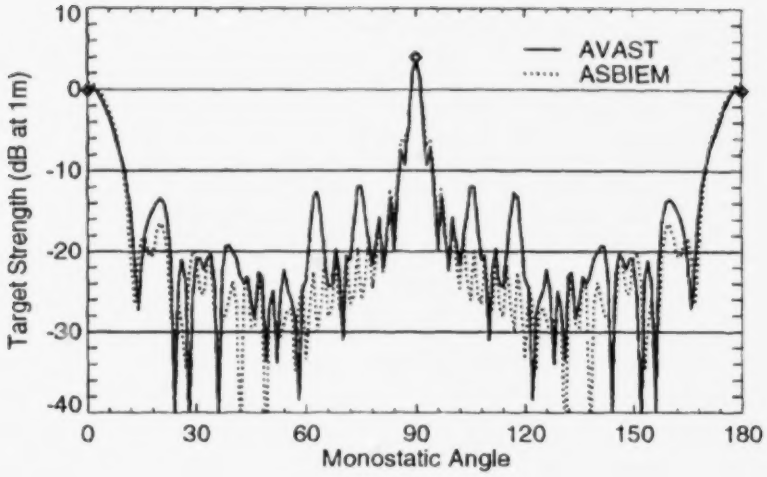


***Figure 15:*** *Monostatic TS of Flat Cylinder - 7.5 kHz*

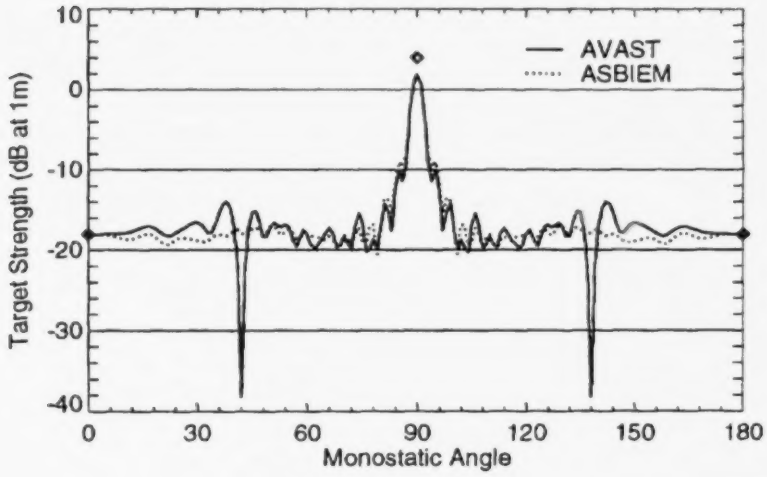


***Figure 16:*** *Monostatic TS of Hemi Cylinder - 7.5 kHz*

The models analysed were those of cylinders of overall length 2.0m and radius 0.25m. The models were examined at three frequencies (2.5 kHz, 5.0 kHz, and 7.5 kHz) in a free-field environment. Results were generated for both the bistatic and full monostatic cases and compared to theoretical results where available.

For the bistatic case, there was generally good agreement between AVAST, ASBIEM, and theoretical results for the specific source locations selected. The results from the cylinder with hemispherical endcaps seem to show better agreement than those from the flat end cylinder, likely due to the sharp geometric changes with the flat end cylinder. Typically all three frequencies showed good agreement indicating that the level of refinement was sufficient. The dominant feature of the bistatic target strength in general was forward scattering which was always the largest amplitude lobe.

For the monostatic analyses, the AVAST and ASBIEM codes showed very good agreement for both the 2.5 kHz and 5 kHz cases for both cylinder models. At the lowest frequency, AVAST seemed to show a slightly better agreement with the theoretical results. At the highest frequency, however, AVAST, while correctly matching the broadside and endfire results and the general level, appears to contain some anomalous side lobes and nulls. In past analyses, these side lobes disappear when a more refined grid is used, so while the bistatic results implied the grid was sufficiently refined, these results indicate this was not the case. At least for the AVAST code, ten elements per acoustic wavelength is not quite sufficient for the complete analysis.

In general, the above comparisons show that AVAST and ASBIEM give comparable results when used to predict rigid target strength. The ASBIEM code runs on the order of one magnitude faster than the AVAST code, but can only be used to model structures which are axisymmetric. Future work on AVAST will concentrate on examining elastic target strength (allowing for internal structure), exploring ways to increase the frequency range (including examining the anomalous lobes demonstrated here), and examining a variety of environmental conditions such as shallow water and varying bottom conditions.

# References

1. Brennan, D.P., Smith, M.J., "Spectral Acceleration Acoustic Modeling and Validation Using AVAST," Martec Ltd., DREA CR 1999-144, 1999.

2. Brennan, D.P., "Acoustic Vibration and Strength Analysis Program (AVAST): Quick User Reference Guide 7.0," Martec Ltd., DREA Contractor Report 97/455, 1997.

3. Brennan, D.P., Chernuka, M.W., "Enhancements to the Capabilities of the AVAST Code," Martec Ltd., DREA Contractor Report 97/456, 1997.

4. Brennan, D.P., Chernuka, M.W., "Enhancement and Validation of the Elasto-Acoustic Capabilities of AVAST," Martec Ltd., DREA Contractor Report 97/457, 1997.

5. Fawcett, J.A., "Finite Element Modelling of Three-Dimensional Scattering from Azimuthally-Symmetric Elastic Shells," SACLANTCEN Report SR-273, February, 1998.

6. Gilroy, L.E., Brennan, D.P., "Predicting Acoustic Target Strength with AVAST," Private Communication, June 2000.

7. Gilroy, L.E., "Numerically Predicted Aspects of Submarine Target Strength," Private Communication, June 2000.

8. Gilroy, L.E., "Boundary Element-Based Predictions of Submarine Target Strength Using AVAST," Private Communication, November, 2000.

9. Urick, R.J., Principles of Underwater Sound, 3rd Edition, McGraw-Hill Book Company, 1983.

10. Pierce, A.D., Acoustics: An Introduction to its Physical Principles and Applications, McGraw-Hill Book Company, 1981.

11. Bradley, M., "Environmental Acoustics Pocket Handbook," 2nd Edition, Planning Systems Inc., Louisiana, March, 1996.

12. Kerr, D.E. (ed.), Propagation of Short Radio Waves, M.I.T. Radiation Laboratory Series, vol. 13, pp. 445-469, McGraw-Hill Book Co., New York, 1951.

13. Dragonette, L.R., Sarkissian, A., Private Communication, April, 1999.

P516761.PDF [Page: 35 of 37]

UNCLASSIFIED
SECURITY CLASSIFICATION OF FORM
(highest classification of Title, Abstract, Keywords)

## DOCUMENT CONTROL DATA

(Security classification of title, body of abstract and indexing annotation must be entered when the overall document is classified)

1 ORIGINATOR (the name and address of the organization preparing the document Organizations for whom the document was prepared, e g Establishment sponsoring a contractor's report, or tasking agency, are entered in section 8 )

Defence Research Establishment Atlantic
P.O. Box 1012
Dartmouth, N.S. B2Y 3Z7

2 SECURITY CLASSIFICATION (overall security classification of the document including special warning terms if applicable)

UNCLASSIFIED

3 TITLE (the complete document title as indicated on the title page Its classification should be indicated by the appropriate abbreviation (S,C,R or U) in parentheses after the title)

Comparison of Three-Dimensional and Axisymmetric Software for Predicting Acoustic Target Strength

4 AUTHORS (Last name, first name, middle initial If military, show rank, e g Doe, Maj John E )

L.E. Gilroy, J. Fawcett

| 5 DATE OF PUBLICATION (month and year of publication of document) | 6a NO OF PAGES (total containing information Include Annexes, Appendices, etc) | 6b NO OF REFS (total cited in document) |
|---|---|---|
| November 2001 | 29 | 13 |

7 DESCRIPTIVE NOTES (the category of the document, e g technical report, technical note or memorandum If appropriate, enter the type of report, e g interim, progress, summary, annual or final Give the inclusive dates when a specific reporting period is covered)

Tech Memo

8 SPONSORING ACTIVITY (the name of the department project office or laboratory sponsoring the research and development Include address)

Defence Research Establishment Atlantic

| 9a PROJECT OR GRANT NO (if appropriate, the applicable research and development project or grant number under which the document was written. Please specify whether project or grant) | 9b CONTRACT NO (if appropriate, the applicable number under which the document was written) |
|---|---|
| 1ga14 | |

| 10a ORIGINATOR'S DOCUMENT NUMBER (the official document number by which the document is identified by the originating activity. This number must be unique to this document ) | 10b OTHER DOCUMENT NOs (Any other numbers which may be assigned this document either by the originator or by the sponsor.) |
|---|---|
| DREA TM 2001-018 | |

11 DOCUMENT AVAILABILITY (any limitations on further dissemination of the document, other than those imposed by security classification)

( X ) Unlimited distribution
( ) Defence departments and defence contractors; further distribution only as approved
( ) Defence departments and Canadian defence contractors; further distribution only as approved
( ) Government departments and agencies; further distribution only as approved
( ) Defence departments; further distribution only as approved
( ) Other (please specify):

12. DOCUMENT ANNOUNCEMENT (any limitation to the bibliographic announcement of this document This will normally correspond to the Document Availability (11). However, where further distribution (beyond the audience specified in (11) is possible, a wider announcement audience may be selected)

Full, unlimited

UNCLASSIFIED
SECURITY CLASSIFICATION OF FORM

P516761.PDF [Page: 36 of 37]



13 ABSTRACT (a brief and factual summary of the document It may also appear elsewhere in the body of the document itself It is highly desirable that the abstract of classified documents be unclassified Each paragraph of the abstract shall begin with an indication of the security classification of the information in the paragraph (unless the document itself is unclassified) represented as (S), (C), (R), or (U) It is not necessary to include here abstracts in both official languages unless the text is bilingual)

Recent work at the Defence Research Establishment Atlantic (DREA) has led to the development of software for predicting the target strength of underwater objects. This capability is incorporated into the general acoustic radiation prediction software tool, AVAST While AVAST has been successfully validated against a limited set of theoretical data, it has not been fully validated against experimental data or other numerical codes. In this report, AVAST predictions are compared to those made by an axisymmetric-based code (ASBIEM) developed at SACLANTCEN for a small cylinder with either flat or hemispherical endcaps. The results were compared at three frequencies for either the full monostatic case or the bistatic case (with three different source locations). For the bistatic case, there was generally good agreement between AVAST, ASBIEM, and theoretical results for the specific source locations selected The results from the cylinder with hemispherical endcaps showed slightly better agreement than those from the flat end cylinder For the monostatic analyses, the AVAST and ASBIEM codes showed very good agreement at the lower frequencies for both cylinder models. At the lowest frequency, AVAST seemed to show a slightly better agreement with the theoretical results At the highest frequency, however, AVAST, while correctly matching the broadside and endfire results and the general level, appears to contain some anomalous side lobes and nulls. In general, the comparisons showed that AVAST and ASBIEM gave comparable results when used to predict rigid target strength The ASBIEM code runs on the order of one magnitude faster than the AVAST code, but cannot be used to model structures which are not axisymmetric.

14 KEYWORDS, DESCRIPTORS or IDENTIFIERS (technically meaningful terms or short phrases that characterize a document and could be helpful in cataloguing the document They should be selected so that no security classification is required Identifiers, such as equipment model designation, trade name, military project code name, geographic location may also be included If possible keywords should be selected from a published thesaurus e g Thesaurus of Engineering and Scientific Terms (TEST) and that thesaurus-identified If it not possible to select indexing terms which are Unclassified, the classification of each should be indicated as with the title)

acoustic
target strength
AVAST
ASBIEM
axisymmetric
mine
underwater
structure
boundary element
acoustic radiation
cylinder
bistatic
monostatic